



Microstructure evolution of Nafion/silica membrane under humidity conditions

Junrui Li ^{a,b}, Haolin Tang ^{a,*}, Zhao Wang ^a, Mu Pan ^a

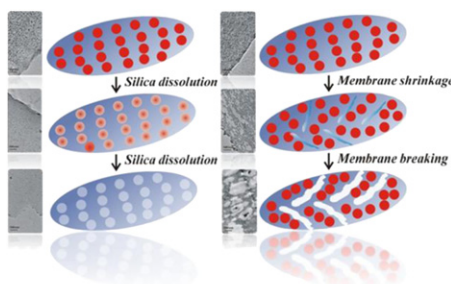
^a State Key Laboratory of Advanced Technology for Materials Synthesis and Processing, Wuhan University of Technology, Wuhan 430070, PR China

^b Department of Chemistry, School of Science, Wuhan University of Technology, Wuhan 430070, PR China

HIGHLIGHTS

- ▶ Microstructure evolution of Nafion/silica membrane under humidity cycles.
- ▶ Silica nanoparticles dissolving in hybrid membrane.
- ▶ Agglomeration of silica nanoparticles in Nafion/silica membrane.

GRAPHICAL ABSTRACT



ARTICLE INFO

Article history:

Received 21 October 2012

Received in revised form

31 January 2013

Accepted 2 February 2013

Available online 9 February 2013

Keywords:

Fuel cell

Water retention proton exchange membrane

Durability

Microstructural degradation

Hydrogen crossover

ABSTRACT

Impregnating hygroscopic nanoparticles, typically silica in Nafion membrane has received intense interest in high-temperature PEMFCs application due to increased water retention ability, proton conductivity and mechanical stability. However, typical Nafion/silica membranes may suffer from potential durability degradation because of the instability of inorganic–organic electrostatic interface under humidifying conditions. Here, we investigate microstructural evolutions of this membrane and the subsequent performance. Aggregation and dissolving of silica nanoparticles and membrane fractures are observed under humidifying and RH cycling tests, thus leading to a significant decay of proton conductivities from $\sim 0.095 \text{ S cm}^{-1}$ to $\sim 0.055 \text{ S cm}^{-1}$ after 720 h of RH cycles. Simultaneously, H_2 crossover soars to nearly 40 times larger than the initial. Inorganic–organic interfaces are recognized to be crucial in the stability and performance of this type of composite membrane. The insight into the degradation process will provide meaningful reference for optimizing composite membranes and designing competent candidates for high-temperature PEMFCs operation.

© 2013 Elsevier B.V. All rights reserved.

1. Introduction

High-temperature working proton exchange membrane fuel cells (PEMFCs) are receiving increasing interest [1–3] due to the benefits of simplified water management, broader gas choices, free from CO poisoning on Pt catalysts and most crucially the lower noble metal use amounts [4]. Thus, higher-temperature membrane has been recognized as one of three key techniques for further

widespread application of PEMFCs [5]. Perfluorosulfonic acid (PFSA) based membranes such as Nafion have been widely known as the state-of-art membrane for PEMFCs due to its high proton conductivity as well as preminent chemical and mechanical stability [6]. However, Nafion membranes are prone to apparently declining in its proton conductivity [7] if exposed to low relative humidity (RH) and elevated temperature conditions, which precludes its application in high-temperature PEMFCs [8,9].

Impregnation of hygroscopic oxide particles such as SiO_2 into the ionic domains of the proton exchange membrane (PEM) to attain hybrid membranes has the potential to alleviate the problems associated with operation under harsh conditions. After the

* Corresponding author. Tel.: +86 27 8788 4448; fax: +86 27 8787 9468.

E-mail addresses: tanghaolin2005@yahoo.com.cn, thln@whut.edu.cn (H. Tang).

pioneering study reported by Mauritz et al. [10], intensive studies [11–13] have been conducted in the development of Nafion/inorganic composite membranes. In the case of Nafion/silica membranes, the hybrid membranes have been regularly achieved by recasting of mixture of silica and Nafion ionomers or by in situ sol–gel reaction of inorganic precursors in the polymer atmosphere [14]. However, the distribution and the interfacial steadiness of silica and Nafion are unsatisfactory since hydrolyzed inorganic precursors like TEOS molecules tend to permeate the Nafion matrix and crosslink together during the longtime sol–gel process. Tang et al. [15] has successfully prepared a homogeneously distributed nanosized silica particles by employing the self-assembly method. The phase separation instinct of Nafion bicontinuous structures drives the silica particles to be confined in the ionic domains [16], thus forming a sharp interface in the composite membranes.

It is essential to recognize the significant role organic–inorganic interface plays in the distribution and phase behavior of hybrid membranes, likewise in the conclusive performance of PEMFCs. Stronger interfacial interaction between the organic and inorganic atmosphere in the self-assembled Nafion/silica membrane [15] leads to tougher tensile strength along with higher durability [17] than that of sol–gel prepared membrane. Tunable properties of the hybrid inorganic–organic interface, including the classes of interactions present, the existence of labile bonds, and the surface energy, make it accessible to modulating the performance of PEM, ranging from mechanical strength [18] to chemical and thermal stability [19], from phase separation to proton conductivity [20,21]. The enhanced performance and specific properties of these hybrid materials result not merely from the combination of the individual component, but also from the solid interface created by the strong synergy [22]. The higher the specific surface area of inorganic fillers, the larger zeta potential and consequently superior power output is [18]. Besides, nanoscopic-sized particles are of greatest interest due to the high surface-to-volume ratios, namely numerous hydrophilic surface groups that may adsorb water molecules [23]. With increasing the surface areas of inorganic fillers, the inorganic nanoparticles get smaller in their sizes and the interfacial synergy become increasingly prevalent, thus determining the properties of the hybrid materials.

In this perspective, it is profitable to control the size of inorganic fillers and to adapt the interfacial interaction between inorganic and organic moieties. Self-assembled Nafion/silica membrane can furnish fine dispersion [24] of inorganic nanoparticles and rather strong interfacial interaction [25], but suffers from potential durability reduction owing to the strain-to-failure limit of this class of composite membranes and swelling induced stress as reported [26]. In addition, high surface energy of the fine-sized nanoparticles may lead to aggregation and harsh interface separation [27], thus causing severe deterioration of membranes and PEMFCs performance [28]. Our previous research revealed that the dimensional change induced by the RH change cycling can be quite large [29]. The early failure of the PEMs (<1000 h) is typically ascribed to the structural failure of the membranes including the cracking, ripping, puncture, humidity-generated stresses [30].

Before either optimizing PEMFCs composite materials further with respect to their durability, or ameliorating system operations and running procedures to preclude the most detrimental conditions, insight into the degradation mechanisms that lead to irreversible performance defeat and the association between the process and the operating conditions, the evolution of the material structures and the impact on fuel cell performance is needed. Particularly, liquid water and dynamic water uptake always present in the PEM fuel cell even operated at low humidity. The variation of humidity induced stress on composite membranes may affect the microstructure of the membrane, leading to the reduced durability

of fuel cells. As far as we have concerned, scarce researches have been developed to investigate the durability and the microstructural transformation of this type of composite membranes [16,31–33] during the fuel cell operation or accelerated process. In this paper, the microstructure evolution of the Nafion/silica composite membranes prepared from self-assembly is observed after different duration time of accelerated relative humidity cycles and hot water resolution treatment. An evident dissolution loss of the silica particles and the membrane decay has been observed. The subsequent performance of the transformed membrane is examined by the single cell tests, electrochemical impedance spectrum and fuel gas permeability through the membranes. The study of the relation between microstructure evolution and the accelerated tests intends to provide reference for designing durable organic/inorganic composite membranes eligible for application in PEMFCs.

2. Experimental section

2.1. Synthesis of the Nafion/silica composite membrane

Nafion ionomers were transferred to N-methyl-2-pyrrolidone solution (NMP, Fluka) by distilling a mixing solution containing 500 mL Nafion DE 520 solution (5 wt% Nafion, 50 ± 3 wt% water and 48 ± 3 wt% 1-propanol, EW is 1000, DuPont) and 500 mL NMP till the solution temperature reached to 203°C to remove water and solvent. Prior to the transferring, the Nafion solution was transformed to Na^+ form by adjusting the pH of the solution to 7.0 with NaOH. Tetraethoxysilane (TEOS, Shanghai Reagent Co., China) was dissolved to 80 mL Nafion/NMP solution using a homogenizer to obtain final 5 wt% SiO_2 in Nafion ionomer. After 5 min, concentrated HCl/water solution (Shanghai Reagent Co., China, 37 wt% HCl, 67 wt % water, which were the pH adjust reactant and hydrolysis material), was added in the mixing solution under vigorous stirring to make $\text{H}_2\text{O}:\text{TEOS}$ ratios of 40:1. After stirred for 8 h, Nafion-stabilized SiO_2 nanoparticles, denoted as Nafion– SiO_2 were obtained.

The Nafion/ SiO_2 nanocomposite membranes were prepared by recasting. The pH of the Nafion– SiO_2 solution was adjusted to 7.0 and the solution was recast using Petri dish, followed by the heat-treatment at 130°C for 5 h and then at 200°C for 3 h. The as-prepared membranes then treated by a standard procedure of 30 min in 5 wt% H_2O_2 solution at 80°C , 30 min in distilled water at 80°C , 30 min in 0.5 M H_2SO_4 solution at 80°C and finally 30 min in distilled water at 80°C again.

2.2. Degradation test of the Nafion/silica composite membranes

The fuel cell was fabricated as follows. First, a catalyst layer consisting of Pt/C (60 wt% Pt/C, Johnson Matthey) and Nafion ionomers was transferred to the membrane surface to obtain a catalyst coated membrane (CCM). Pt catalyst loadings of both electrodes were 0.2 mg cm^{-2} , and the dry loadings of Nafion were 0.4 mg cm^{-2} . The gas diffusion layer (GDL) was placed on the anode and cathode side of the CCM to form a membrane-electrode assembly (MEA). The MEA was mounted in a single cell test fixture with a serpentine flow field and a fuel cell clamp (with an active area of 25 cm^2).

The durability of the composite membranes was investigated at accelerated RH cyclic tests and hot water resolution tests. In case of hot water resolution tests, hot water was fed to the cell 80°C to investigate the membrane solubility under high humidity conditions. In case of the accelerated RH cyclic tests, absolute dry H_2 and air were fed to the cell for 8 min, followed by 100 RH% H_2 and air for another 2 min at 80°C . The RH was changed every 10 min.

Microstructures and element mapping of the Nafion/SiO₂ samples were characterized by high-resolution TEM (HRTEM, JEM-2010FEF) equipped with an energy dispersive X-ray spectroscopy (EDS) detector. For the sample preparation, a piece of the Nafion/silica membrane was sliced by an ultramicrotome (Leica Ultracut UCT) using a diamond knife at room temperature. The thickness of the sample was about 20–40 nm. The sliced specimen was supported on a conventional Cu mesh with a carbon micro-grid.

The SiO₂ content in the Nafion/SiO₂ membrane was tested by inductively coupled plasma atomic emission spectrometry (ICP-AES) measurement (type PerkinElmer, Optima 4300DV, American). For preparing the samples, 1 g Nafion/silica sample and 0.5 g NaOH powder were sintered in corundum crucible at 900 °C for 1 h. Then the mixing powder was dissolved in deionized water. After filtration, the filtrate volume was finally set to 1000 mL by deionized water.

The characteristics of the SiO₂ nanoparticles in the Nafion/SiO₂ membranes and that of pure Nafion membrane were examined by a Fourier transform infrared spectroscopy-attenuated total reflectance (FTIR-ATR) (Nicolet Avatar-370) system with a resolution of 2 cm⁻¹. A ZnSe crystal was used as the ATR plate with an incidence angle of 45°.

2.3. Electrochemical test of the Nafion/silica composite membranes

The single PEM fuel cell performances of the Nafion/silica membrane and Nafion 212 membrane were tested on G50 Fuel Cell Test Station (GreenLight) at 60–95 °C without back pressure, using H₂ as the fuel, and air as the oxidant. The H₂ and air flow rates were 300 and 2000 sccm, respectively. The humidity of the H₂ and air was kept at the same level and the cell performance was measured as a function of relative humidity (RH). Prior to measurement, cells were activated by polarization at a constant current until stable performance was reached.

An Autolab PG30/FRA analyzer was used to perform Electrochemical Impedance Spectrum (EIS). AC perturbations were applied on electronic load in order to make current oscillating with AC component for a given DC bias. The ratio of AC to DC amplitude was 0.03. The AC frequency was scanned over the range of 60 kHz–1 Hz.

The gas permeability or crossover through membranes was assessed by measuring diffusion-limited hydrogen oxidation current densities of the crossover H₂ using Autolab PG30/FRA. H₂ gas (300 sccm) was fed to the anode side of the cell while N₂ was fed to the cathode. By applying a dynamic potential from 0 to 0.7 V vs. the anode (i.e., dynamic hydrogen electrode, DHE) at 0.5 mV s⁻¹, the limiting H₂ oxidation current density was measured. The anode side, where hydrogen evolution takes place, served as the counter electrode and the DHE reference electrode.

3. Results and discussion

3.1. Electrochemical characterization of Nafion/silica membrane

As evidenced by our previous work [25], Nafion/silica composite membrane with a homogenous distribution of inorganic nanoparticles and a relatively strong interfacial collaboration has been attained through the self-assembly technique. The presence of fine-sized and uniformly distributed silica nanoparticles endues the composite membrane with increased water retention capability even at low RH and high temperature above 80 °C [13], thus resulting in a lower proton conductive resistance and subsequent enhanced single cell performance of the composite membrane compared to that of pristine Nafion 212 membrane. As displayed in Fig. 1a, the polarization curves of the self-assembled Nafion/silica

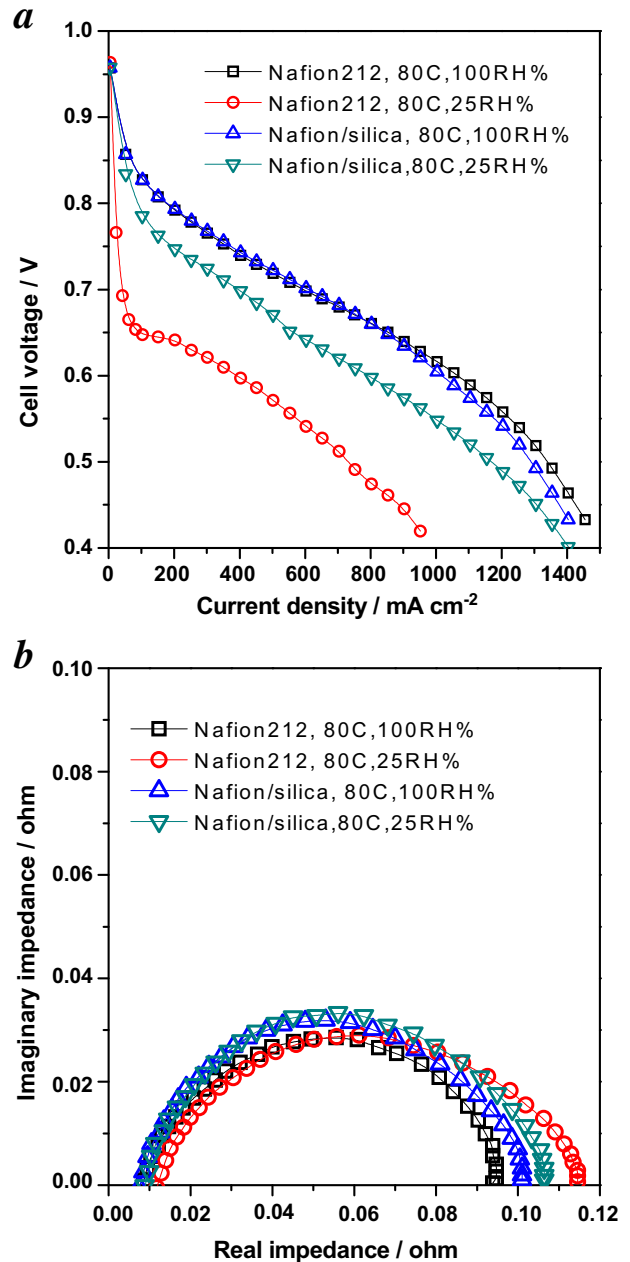


Fig. 1. (a) H₂–air performance of the PEMFCs equipped with Nafion 212 membrane and Nafion/silica membrane tested at 100% RH and 25% RH under 80 °C, respectively. (b) EIS spectra of Nafion 212 and Nafion/silica membrane observed at 100% RH and 25% RH under 80 °C.

membrane and the pristine Nafion 212 membrane are obtained at 100% RH and 25% RH under 80 °C, respectively. The performance of PEMFCs equipped with these two membranes is nearly congruent. While at 25% RH under 80 °C, PEMFCs equipped with pure Nafion membrane endures drastic power output decay when initially starting the test. The rapid decay is clearly ascribed to the dehydration of the membrane because of the inferior water retaining ability [34]. In contrast, PEMFCs with Nafion/silica membrane exhibits a greatly stable performance with a minor degradation when RH drops from 100% to 25%. Although the water uptake has been raised under low RH, incorporation of silica nanoparticles with extremely low proton transport ability [35] will result in a slight decrease in proton conductivity compared to fully humidified pure Nafion membrane, which is consistent with the slightly lower

single cell performance of Nafion/silica membrane than that of Nafion 212 membrane.

Electrochemical impedance spectra of both Nafion/silica membrane and Nafion 212 on a Nyquist illustration are characterized by a nearly perfect semi-circle (Fig. 1b). The left side junction of the impedance curves with the substantive axis is attributed to the total ohmic resistance of the cell (R_Ω), which is dominated by the membrane resistance. The impedance value of Nafion/silica membrane tested at both 100% RH and 25% RH under 80 °C and that of Nafion 212 membrane examined at 100% RH under 80 °C are almost equivalent and difficult to differentiate on the scale of this graph. Nevertheless, it is notable that Nafion 212 membrane presents the highest resistance resulted from the low RH. The value of right side intersection of impedance curves with the real axis is symbolized as R_p , which stands for the polarization resistance and can be employed to provide information about the changes caused by dehydration of Nafion [36]. The R_p values are observed in the following order: Nafion 212 membrane at 25% RH > Nafion/silica membrane at 25% RH > Nafion/silica membrane at 100% RH > Nafion 212 membrane at 100% RH, which is in good consistence with the single cell performance results. At constant overpotential, the relationship of the area resistance contributed by polarization r_p and the apparent value of the charge transfer resistance (r_p^o)_{app} is shown as Equation (1):

$$r_p = (r_p^o)_{\text{app}} \exp\left(\frac{-\eta}{b}\right) \quad (1)$$

where η represents the cathode overpotential that is constant in the present test and b represents the Tafel slope $b = RT/(\alpha nF)$ with α representing the charge transfer coefficient and n symbolizing the quantity of electrons transferred in the rate-determining step. Both mass transport and ohmic overpotential are small enough to be neglected because the potential exerted during the EIS test is very close to the open circuit potential (OCP). Therefore the overpotential is determined by the charge transfer term and the r_p depends on $(r_p^o)_{\text{app}}$, the latter value is pertinent to the apparent exchange current density $(i_p^o)_{\text{app}}$ according to Equation (2).

$$(r_p^o)_{\text{app}} = \frac{RT}{nF(i_p^o)_{\text{app}}} \quad (2)$$

The apparent exchange current density $(i_p^o)_{\text{app}}$ was calculated from Equation (3), where i^o represents the intrinsic current density and the S_{act} stands for the electrocatalytically active surface area.

$$(i_p^o)_{\text{app}} = i^o S_{\text{act}} \quad (3)$$

On the basis of Equations (1)–(3) [37] it is probable that the alternation of R_p with the RH reflects the apparent activity of the

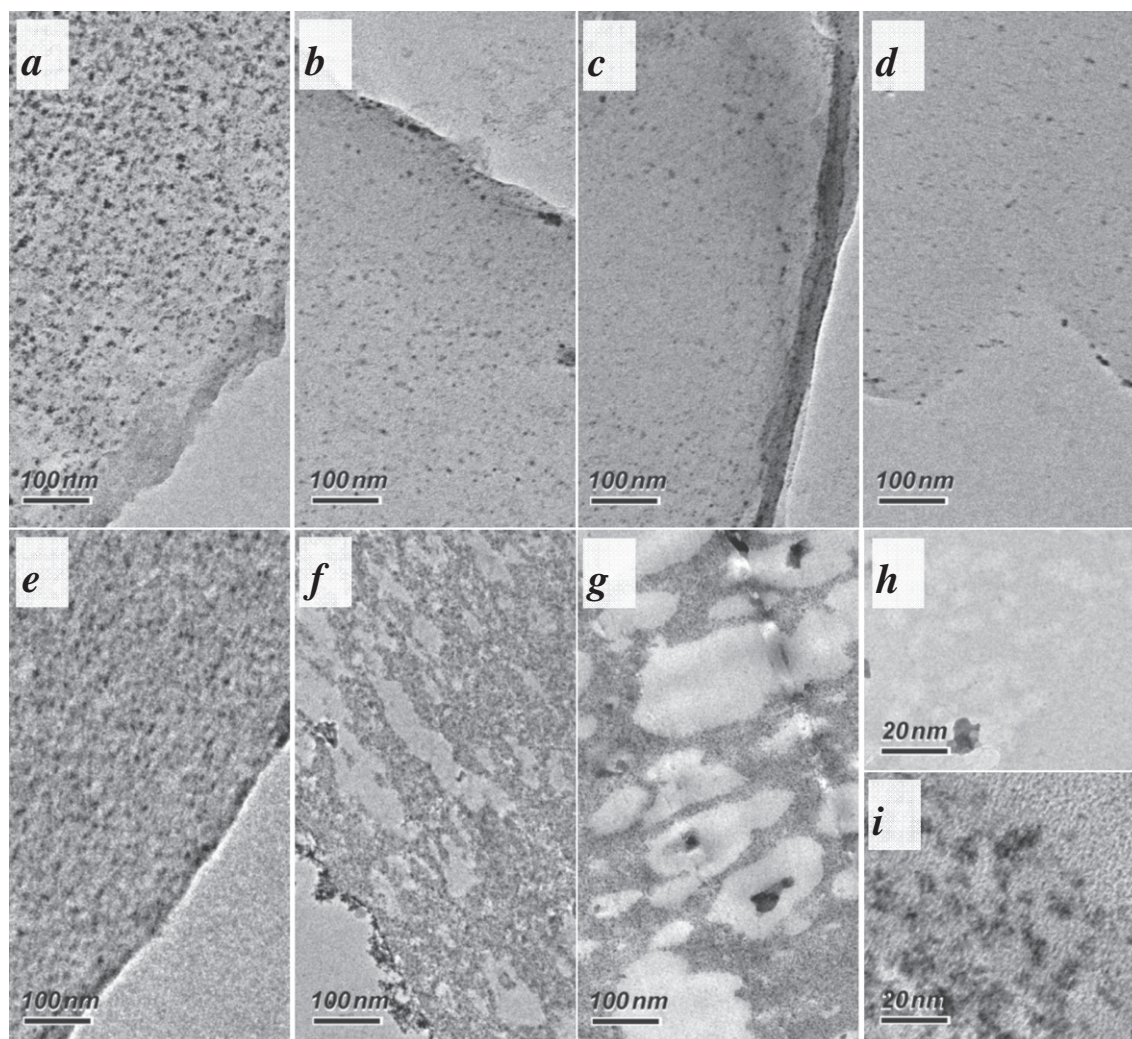


Fig. 2. TEM images of (a) as-prepared Nafion/silica membrane, (b–d) hot-water solubility 96, 148 and 240 h, (e–g) humidity cycles 240, 480, and 720 h, (h) enlarged image of (d), (i) enlarged image of (g).

cathode and the charge transport activity. The availability of protons involved in the electrode reaction is responsible for the difference in charge transfer resistance. In a pure Nafion electrolyte, the proton conductivity was significantly decreased by dehydration, therefore leading to the difficulty of obtaining protons in the catalyst layer, which was reflected in a lower $(i_p^0)_{app}$ and ultimately larger $(r_p^0)_{app}$. The catalyst layer assembled with the same catalyst but with different proton conductors providing distinct proton availabilities will result in significantly different S_{act} and consequently different $(i_p^0)_{app}$, as demonstrated by Russell Kunz et al. [38]. Pure Nafion electrolyte endures a rather larger decrease in proton conductivity compared to Nafion/silica electrolyte under dehydration. Hence the charge transfer dearth in the membrane assembly electrolyte (MEA) resulted from the dehydration becomes a significant bottleneck of the whole cell performance.

3.2. Microstructural characterization and degradation tests of composite membrane

Fig. 2 displays the TEM images of microstructural evolution from the as-prepared Nafion/silica membrane to the degraded membrane after hot-water treatment and accelerated RH cycles. Soluble phenomenon of silica nanoparticles incorporated in the composite membrane was observed with extracting the membrane alternately from the hot water treatment with various lasting time of 96, 148 and 240 h, respectively. It is significantly obvious that the impregnated silica nanoparticles (black dots) gradually vanish and shrink in their sizes among the randomly selected field of vision with prolonging the treating spell. After 240 h of hot-water treatment, the silica nanoparticles can hardly be captured and transform into apparently minuscule dots with an obscure morphology in the TEM graph scaled at 100 nm, thus indicating the Nafion/silica composite membrane may probably suffer from severe silica losses and are not sufficiently stable under high temperature operation. In addition, as presented in Fig. 2e–g and Fig. 2i, apparent microcracks in membranes were generated and intense aggregation of well-distributed silica nanoparticles were observed after the RH cycles test. Our previous work showed that significant shrinkage stress (3.1 MPa) and dimensional change of Nafion membrane can be induced by RH cycling [39]. The longtime periodic shrinkage stress would result in the membrane cracking, as obviously shown in Fig. 2h. The degradation process of the Nafion/silica composite membranes is the synergistic result of silica particles leakage, aggregation and RH cycles-induced membrane cracking.

ICP-AES test was employed to study the contents of silica particles in the Nafion/silica composite membrane. Fig. 3 shows the time-dependent variation of silica contents after hot-water treatment of 240 h and RH cycles of 720 h. The silica content in the hot-water-washed Nafion/silica membrane shows a considerable decrease from the initial 5 wt% to 1.37 wt% after 240 h. This result solidly proves the dissolving process observed in Fig. 2a–d. The inherent ionic clusters will significantly swell in size and tend to interconnect with each other to form water channels when Nafion/silica composite membranes were exposed to humidified atmosphere [40]. The hydrophilicity of silica particles will further prompt the water sopping of the membranes. Under hot-water treatment, the swollen ionic clusters and increased mobility of Nafion polymer contribute to the leakage of silica particles. In contrast, the silica content in Nafion/silica membranes treated with RH cycles presents a slight reduction from the initial 5 wt% to 3.54 wt% after 720 h. However, it is noticeable that cyclical swelling and shrinking behaviors of Nafion membranes induced by the RH-cycles can lead to the attenuation of interactions between silica particles and the ionic clusters. The attenuated interaction should be responsible for the silica particles leakage and their migration through the water channels to

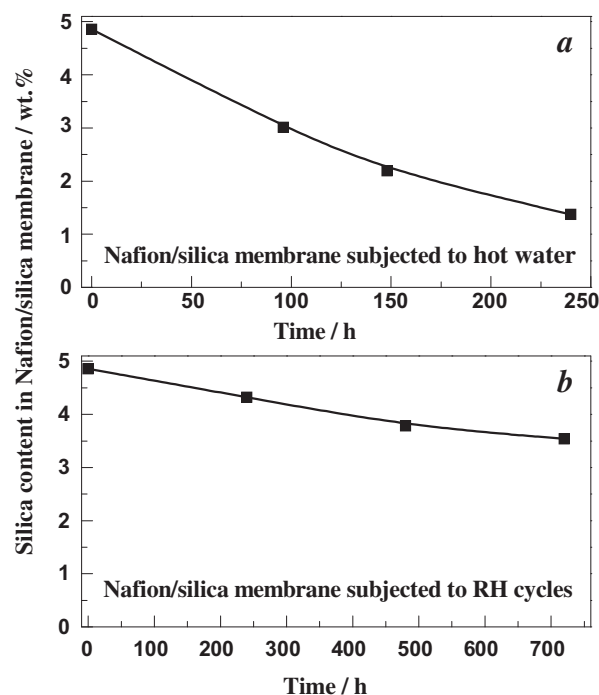


Fig. 3. Time-dependent variation of silica contents in Nafion/silica membrane subjected to hot water (a) and to RH cycles (b), respectively.

aggregate into larger ones, as shown in Fig. 2i. The leakage of silica particles was also demonstrated by the EDS analysis and random element mapping shown in Fig. 4. In the Si element mapping of Nafion/silica membrane treated in hot water for 240 h, the number of Si elements decreases evidently, while no obvious changes were observed in the mapping scope of the membrane treated with RH cycles. After RH cycles of 720 h, the slight decline in the relative peak intensity of Si element to that of the typical elements in Nafion according to the EDS analysis is consistent with the ICP-AES results.

The characteristics of silica particles in the Nafion/silica membranes and the interaction between silica particles and the sulfonic groups were examined by the FTIR-ATR. Fig. 5 shows the FTIR-ATR spectra of the Nafion/SiO₂ composite membranes after subtracting from that of the pure Nafion membrane. As shown in the figure, four absorption bands at ~ 814 , 947 , 1043 , and 1082 cm⁻¹ appearing in the spectra can be assigned to Si–O–Si asymmetric stretching $\Delta_{asym}(\text{Si–O–Si})$, Si–OH stretching $\Delta(\text{Si–OH})$, Si–O–Si asymmetric stretching $\Delta_{asym}(\text{Si–O–Si})$ of linear configuration, and $\Delta_{asym}(\text{Si–O–Si})$ of cyclic configuration, respectively. Interestingly, a slight shift of the Si–OH stretching peak from the original lower wavenumber of ~ 940 cm⁻¹ (reported by Hagihara, Hiroki et al. [41]) to the higher of ~ 947 cm⁻¹ may imply the formation of R–SO₃H–SiO₂ bond since the attachment of sulfonic groups to the surface of silica would increase the electronic density of Si–OH. The clearly declined reflectance intensity of typical silica peaks indicates reduction in silica content after 240 h hot-water treatment and 720 h RH cycles. In contrast, a slight shift in wavenumber of the peak representing the formed R–SO₃H–SiO₂ bonds from ~ 947 cm⁻¹ in the as-prepared membrane to ~ 945 cm⁻¹ in both the degraded membranes was observed, which was probably due to the attenuated R–SO₃H–SiO₂ bonding strength. It is difficult to judge the change in peaks of SO₃H because the silica content in the membrane is very low (silica ≤ 5 wt%, Nafion ≥ 95 wt%) and correspondingly the concentration of R–SO₃H–SiO₂ is much lower than that of R–SO₃H. Additionally, the typical peaks of Nafion and silica in the composite membranes severely interrupt with each other, making it hardly

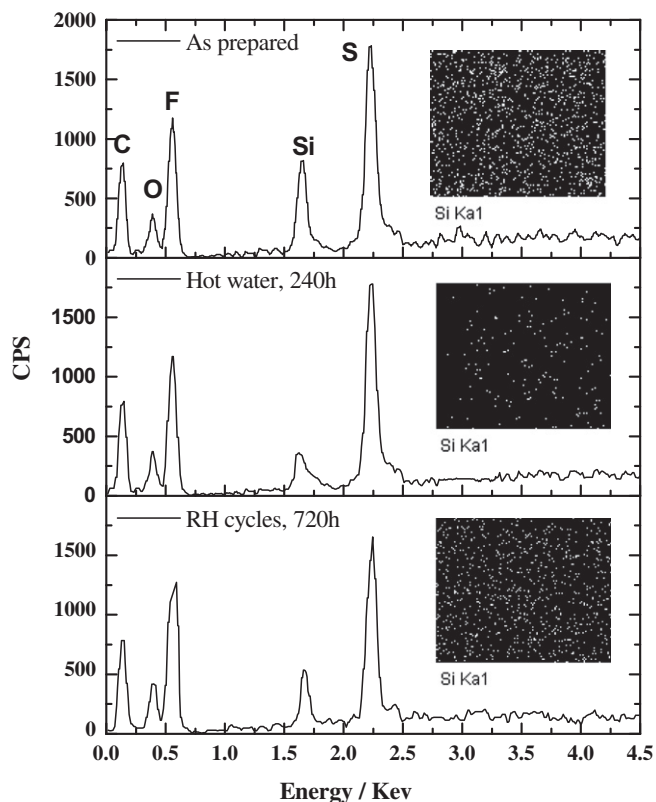


Fig. 4. EDS analysis and Si distribution mapping in the as-prepared Nafion/silica membrane and degraded Nafion/silica membrane subjected to hot water (for 240 h) and to RH cycles (for 720 h), respectively.

discernible. According to the dropped Si–OH stretching peak intensity and the slight shift in peaks of R–SO₃H–SiO₂ bonds, it may be the case that the interplay of some silica particles and sulfonic groups exists in the degraded membrane, but endures a total decrease in bonding sites number and the strength, thus reflecting a weakened interaction between silica fillers and Nafion polymers in general.

Silica nanoparticles are theoretically impregnated into the spherically ionic clusters of the Nafion matrix and established a durable core–shell structure in the membrane under mild situation. The formed R–SO₃H–SiO₂ bonds on the SiO₂ surface with the sulfonic groups on the side chains of Nafion ionomers would be disentangled into R–SO₃H and HO–Si–O when fully saturated

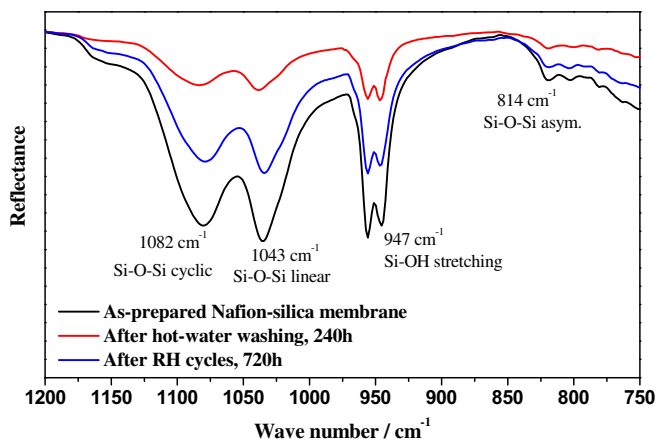


Fig. 5. FTIR spectra of the as-prepared Nafion/silica membrane, degraded Nafion/silica membranes after hot water washing of 240 h and that degraded after RH cycles of 720 h.

under elevated temperature, resulting in separation of the inorganic and organic phase, along with silica leakage. The prolific hydroxyl groups on the surface of silica nanoparticles and the presence of the ionic couple (R–SO₃H–SiO₂) in the inorganic–organic interface are essential for rapid proton hopping by Grotthuss transport [42]. Sel et al. [43] reported that excessive swelling of silica/polymer hybrid membranes with plethoric –SO₃H and –OH groups in water at room temperature would drop proton conductivity at high temperature. Therefore the number of –SO₃H and –OH groups in the interfacial domains should be controlled. The silica solubility also weakens the participation of SiO₂ in proton conduction of the composite membrane and decrease the water retention ability. The influence of membrane cracking and pinholes formation on the whole membrane performance was further demonstrated by the EIS and H₂ crossover measurements.

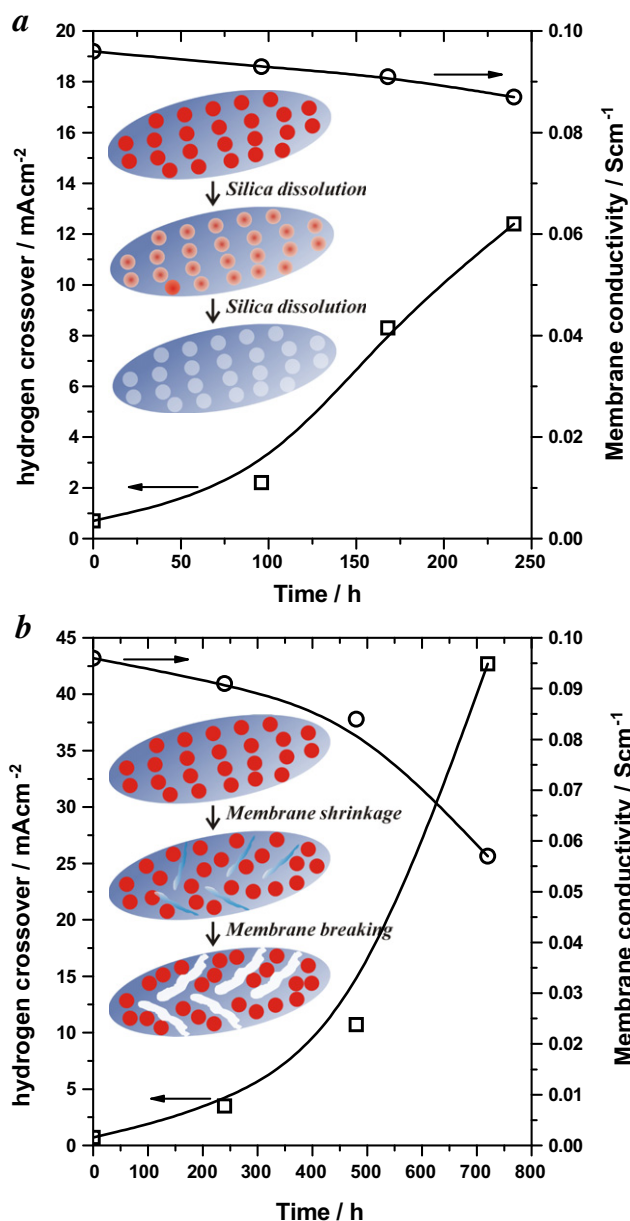


Fig. 6. Hydrogen crossover and membrane proton conductivity of Nafion/silica composite membrane at 100% RH under 80 °C. (a) After hot-water treatment with various time, 96, 148 and 240 h, the inset is a schematic of the dissolving process of silica nanoparticles, (b) after RH cycles tests with increasing persistent time, 240, 480, and 720 h, the inset is a schematic of the membrane degradation process during RH cycles tests.

The absence of the silica nanoparticles may also create pinholes and accessible pathways for gas feeding. As displayed in Fig. 6a, the silica leakage also results in a slight reduction in the membrane proton conductivity and a sharp zoom of the hydrogen crossover with the limiting H_2 oxidation current density peaking at about 13 mA cm^{-2} , more than ten times of the origin value for untreated membrane. Because the water retention ability and the proton conductivity of Nafion/silica composite membranes are highly dependent on the morphology of the interfacial state, the swelling of the membrane and silica losses will definitely damage the interfacial interaction and then lead to the decline in the water uptake and proton conductivity.

The considerable swelling of ionic clusters in Nafion matrix under fully humidified condition subsequently weakens the interfacial interaction between the silica and the Nafion matrix. The dispersion state and morphology of inorganic fillers in the Nafion matrix are closely related to the nature of hydrophilic ionic clusters. Enlarged Nafion ionic clusters and damaged interface fail to bind silica tightly, hence the free-bonded silica nanoparticles tend to agglomerate into larger size in order to reduce the high surface energy [44,45]. The synergy of interfacial separation of Nafion-silica and the RH generated stress of Nafion membrane can accelerate the degradation of the composite membrane. The anchored silica nanoparticles on the side chains of Nafion ionomer would increase its roughness and decrease its mobility as well as elasticity, which may make the hybrid membrane more fragile and easy to break on a macroscopic scale. Fig. 6b presents the severely declined proton conductivity of Nafion/silica membrane and soared H_2 crossover with prolonging the duration of RH cycling. The high resistance of the decayed composite membrane is ascribed to the aggregated silica nanoparticles and the disconnection of proton channels occurred in the cracked membrane. After about 700 h RH cycles, proton conductivity drops down to the value of about 0.055 S cm^{-1} and the limiting H_2 oxidation current density reaches a terrible $\sim 43 \text{ mA cm}^{-2}$, which can lead to shut down and is very dangerous in a running fuel cell.

4. Conclusions

Evident silica dissolving and membrane cracking of degraded Nafion/silica membrane was observed in TEM images. The decrease in silica contents of the composite membranes and the declined interaction between silica particles and sulfonic groups in Nafion were further confirmed by ICP-AES and FTIR-ATR, respectively. Nafion/silica membrane undergoes significant microstructural degradation and subsequently deteriorated proton transportation and severe gas permeability through the membrane in liquid water or under RH cycles. The degradation process of Nafion/silica composite membrane is the synergistic result of silica particles dissolving and aggregation and membrane cracking induced by the hot-water treatment and RH cycles, respectively. Therefore, to design a highly durable Nafion/inorganic particles composite membrane without sacrificing its performance and put forward its application in PEMFCs, two mainly guidelines are needed to follow:

- (1) To decrease the water solubility of the widely used inorganic particles by surface modification or use alternative particles with better water dissolving endurance.
- (2) To solidify the Nafion/particles interface by imposing powerful binding interaction like chemical bonds on the interface and decrease the humidity-induced stress.

Acknowledgment

This work is financially supported by the National Nature Science Foundation of China (51272200), Program for New Century

Excellent Talents in University (NCET-12-0911) and Wuhan “Chengguang” Project (201150431089).

References

- [1] S.-Y. Lee, A. Ogawa, M. Kanno, H. Nakamoto, T. Yasuda, M. Watanabe, *Journal of the American Chemical Society* 132 (2010) 9764.
- [2] V. Di Noto, E. Negro, J.-Y. Sanchez, C. Iojoiu, *Journal of the American Chemical Society* 132 (2010) 2183.
- [3] R. Kannan, P.P. Aher, T. Palaniselvam, S. Kurungot, U.K. Kharul, V.K. Pillai, *The Journal of Physical Chemistry Letters* 1 (2010) 2109.
- [4] V. Di Noto, E. Negro, R. Gliubizzi, S. Lavina, G. Pace, S. Gross, C. Maccato, *Advanced Functional Materials* 17 (2007) 3626.
- [5] S. Chu, A. Majumdar, *Nature* 488 (2012) 294.
- [6] K.A. Mauritz, R.B. Moore, *Chemical Reviews* 104 (2004) 4535.
- [7] P.W. Majsztrik, M.B. Satterfield, A.B. Bocarsly, J.B. Benziger, *Journal of Membrane Science* 301 (2007) 93.
- [8] H.W. Zhang, P.K. Shen, *Chemical Reviews* 112 (2012) 2780.
- [9] H. Zhang, P.K. Shen, *Chemical Society Reviews* 41 (2012) 2382.
- [10] K.A. Mauritz, *Materials Science and Engineering: C* 6 (1998) 121.
- [11] Z. Chai, C. Wang, H. Zhang, C.M. Doherty, B.P. Ladewig, A.J. Hill, H. Wang, *Advanced Functional Materials* 20 (2010) 4394.
- [12] W. Han, K.L. Yeung, *Chemical Communications* 47 (2011) 8085.
- [13] K.T. Adjemian, R. Dominey, L. Krishnan, H. Ota, P. Majsztrik, T. Zhang, J. Mann, B. Kirby, L. Gatto, M. Velo-Simpson, J. Leahy, S. Srinivasan, J.B. Benziger, A.B. Bocarsly, *Chemistry of Materials* 18 (2006) 2238.
- [14] R.C. Jiang, H.R. Kunz, J.M. Fenton, *Journal of Membrane Science* 272 (2006) 116.
- [15] H.L. Tang, M. Pan, *Journal of Physical Chemistry C* 112 (2008) 11556.
- [16] M.K. Mistry, N.R. Choudhury, N.K. Dutta, R. Knott, Z.Q. Shi, S. Holdcroft, *Chemistry of Materials* 20 (2008) 6857.
- [17] V. Di Noto, R. Gliubizzi, E. Negro, G. Pace, *Journal of Physical Chemistry B* 110 (2006) 24972.
- [18] Z. Wang, H. Tang, M. Pan, *Journal of Membrane Science* 369 (2011) 250.
- [19] R. Borup, J. Meyers, B. Pivovar, Y.S. Kim, R. Mukundan, N. Garland, D. Myers, M. Wilson, F. Garzon, D. Wood, P. Zelenay, K. More, K. Stroh, T. Zawodzinski, J. Boncella, J.E. McGrath, M. Inaba, K. Miyatake, M. Hori, K. Ota, Z. Ogumi, S. Miyata, A. Nishikata, Z. Siroma, Y. Uchimoto, K. Yasuda, K.-i. Kimijima, N. Iwashita, *Chemical Reviews* 107 (2007) 3904.
- [20] L. Ghassemzadeh, G. Pace, V. Di Noto, K. Muller, *Physical Chemistry Chemical Physics* 13 (2011) 9327.
- [21] C. Laberty-Robert, K. Valle, F. Pereira, C. Sanchez, *Chemical Society Reviews* 40 (2011) 961.
- [22] C. Sanchez, B. Julian, P. Belleville, M. Popall, *Journal of Materials Chemistry* 15 (2005) 3559.
- [23] V. Di Noto, N. Boaretto, E. Negro, G. Pace, *Journal of Power Sources* 195 (2010) 7734.
- [24] M. Pan, H.L. Tang, S.P. Jiang, Z.C. Liu, *Electrochemistry Communications* 7 (2005) 119.
- [25] H. Tang, S. Wang, M. Pan, S.P. Jiang, Y. Ruan, *Electrochimica Acta* 52 (2007) 3714.
- [26] M.B. Satterfield, P.W. Majsztrik, H. Ota, J.B. Benziger, A.B. Bocarsly, *Journal of Polymer Science Part B: Polymer Physics* 44 (2006) 2327.
- [27] J. Noack, L. Schmidt, H.-J. Glaeser, M. Bauer, E. Kemnitz, *Nanoscale* 3 (2011) 4774.
- [28] Y. Patil, S. Sambandam, V. Ramani, K. Mauritz, *Journal of the Electrochemical Society* 156 (2009) B1092.
- [29] H. Tang, P. Shen, S.P. Jiang, W. Fang, P. Mu, *Journal of Power Sources* 170 (2007) 85.
- [30] F.A. de Bruijn, V.A.T. Dam, G.J.M. Janssen, *Fuel Cells* 8 (2008) 3.
- [31] M.M. Hasani-Sadrabadi, E. Dashtimoghaddam, F.S. Majedi, K. Kabiri, N. Mokarram, M. Solati-Hashjin, H. Moaddel, *Chemical Communications* 46 (2010) 6500.
- [32] A. D'Epifanio, M.A. Navarra, F.C. Weise, B. Mecheri, J. Farrington, S. Licoccia, S. Greenbaum, *Chemistry of Materials* 22 (2010) 813.
- [33] V. Di Noto, N. Boaretto, E. Negro, G.A. Giffin, S. Lavina, S. Polizzi, *International Journal of Hydrogen Energy* 37 (2012) 6199.
- [34] V.A. Sethuraman, J.W. Weidner, A.T. Haug, L.V. Protsailo, *Journal of the Electrochemical Society* 155 (2008) B119.
- [35] M. Nogami, Y. Abe, *Physical Review B* (1997) 12108.
- [36] M. Ciureanu, R. Roberge, *The Journal of Physical Chemistry B* 105 (2001) 3531.
- [37] M. Ciureanu, *Journal of Applied Electrochemistry* 34 (2004) 705.
- [38] H. Xu, H.R. Kunz, L.J. Bonville, J.M. Fenton, *Journal of the Electrochemical Society* 154 (2007) B271.
- [39] H. Tang, M. Pan, F. Wang, P.K. Shen, S.P. Jiang, *Journal of Physical Chemistry B* 111 (2007) 8684.
- [40] K. Schmidt-Rohr, Q. Chen, *Nature Materials* 7 (2008) 75.
- [41] H. Hagihara, H. Uchida, M. Watanabe, *Electrochimica Acta* 51 (2006) 3979.
- [42] R.A. Horne, *Nature* 202 (1964) 1221.
- [43] O. Sel, A. Soules, B. Ameduri, B. Boutevin, C. Laberty-Robert, G. Gebel, C. Sanchez, *Advanced Functional Materials* 20 (2010) 1090.
- [44] B. Park, Y.J. Kim, S. Graham, E. Reichmanis, *ACS Applied Materials & Interfaces* 3 (2011) 3545.
- [45] B. Reeja-Jayan, A. Manthiram, *ACS Applied Materials & Interfaces* 3 (2011) 1492.